*Key Engineering Materials*
*ISSN: 1662-9795, Vol. 926, pp 1188-1194*
*doi:10.4028/p-9i8j3o*

*Submitted: 2021-12-08*
*Revised: 2022-01-26*
*Accepted: 2022-01-26*
*Online: 2022-07-22*

# Non-Uniform Effect of the Contact Conditions on the Earing Profile in Cylindrical Cups of Anisotropic Materials

D.M. Neto[1,a*], M.C. Oliveira[1,b], R.E. Dick[2,c], J.L. Alves[3,d] and L.F. Menezes[1,e]

[1]CEMMPRE, Department of Mechanical Engineering, University of Coimbra, Pinhal de Marrocos, 3030-788 Coimbra, Portugal

[2]Kaiser Aluminum, 859 White Cloud Road, New Kensington, PA 15068, Pennsylvania, USA

[3]Microelectromechanical Systems Research Unit, University of Minho, Campus de Azurém, Guimarães, 4800-058, Portugal

[a]diogo.neto@dem.uc.pt, [b]marta.oliveira@dem.uc.pt, [c]robert.dick@kaiseraluminum.com, [d]jlalves@dem.uminho.pt, [e]luis.menezes@dem.uc.pt

**Keywords:** Cup earing; Friction forces; Material anisotropy; Numerical simulation

**Abstract.** The earing profile of cylindrical cups is mainly dictated by the in-plane anisotropic behavior of the metal sheet. Nevertheless, for materials with a strong anisotropic behavior the contact conditions between the blank and the blank-holder can also affect the material flow due to the non-uniform distribution of the contact forces. The main objective of this study is to numerically assess the influence of the friction conditions on the cup earing profile using the AA3104 aluminum alloy. The strong anisotropy of the *r*-values of this material leads to a non-uniform thickness distribution along the circumferential direction of the flange, resulting in increased thickening in the transverse direction. The effect of the friction coefficient on the earing profile is approximately 4 times larger in the transverse direction than in the rolling direction.

## Introduction

The anisotropic behavior of the materials used in deep drawing operations leads to the formation of ears in cylindrical cups. The earing profile is mainly dictated by the in-plane anisotropy, i.e. the in-plane distribution of both the *r*-values and the yield stresses [1]. That is the reason the earing profile is commonly used to evaluate the performance of constitutive models, namely the yield criteria [2]. Nevertheless, it is consensual that the frictional contact conditions between the blank and the blank-holder can also affect the material draw-in [3]. For example, in case of isotropic materials, an increase of friction leads to a cup with an increased height. In case of anisotropic materials, there is a non-uniform distribution of the contact forces in the cup flange, which changes the material flow asymmetrically along the circumferential direction. Thus, the accurate prediction of the earing profile requires knowledge about the friction conditions in the flange of the cup. Increasing the friction coefficient will also yield a global increase of the cup height, but the change along the circumferential direction depends on the contact pressure distribution under the blank-holder.

The main objective of this study is to numerically assess the influence of the friction conditions on the cup earing. The aluminum alloy AA3104 is adopted in the present analysis due to the highly anisotropic behavior defined by a strong in-plane variation of the Lankford coefficients (*r*-values). The material orthotropic plastic behavior is modelled with an advanced non-quadratic yield criterion, which is compared with the von Mises yield function. Additionally, different values of the friction coefficient are used in the classical Coulomb law.

## Numerical model

The deep drawing of a cylindrical cup is the example selected in this study to highlight the effect of the contact conditions on the earing profile. The geometry of the forming tools is presented in Fig. 1 (a), as well as the critical dimensions. The blank used has an initial thickness of 0.58 mm and a diameter of 76.2 mm and has mechanical properties of an AA3104 aluminum alloy. The forming

process comprises two phases: (i) closing of the blank-holder until attaining a prescribed force of 6 kN; (ii) punch displacement of 25 mm (full drawing) while the blank-holder force increases linearly (0.085 kN/mm of punch displacement).

The numerical simulations are performed with the in-house finite element code DD3IMP [4]. Only one-quarter model is simulated due to the geometry and material symmetry conditions. The forming tools are assumed rigid and modelled by Nagata patches [5], as shown in Fig. 1 (b). The friction forces between the forming tools and the blank are described by the classical Coulomb friction law, considering a constant friction coefficient. The blank was discretized with linear hexahedral finite elements, using two layers of elements through thickness, leading to a total of 13282 finite elements.

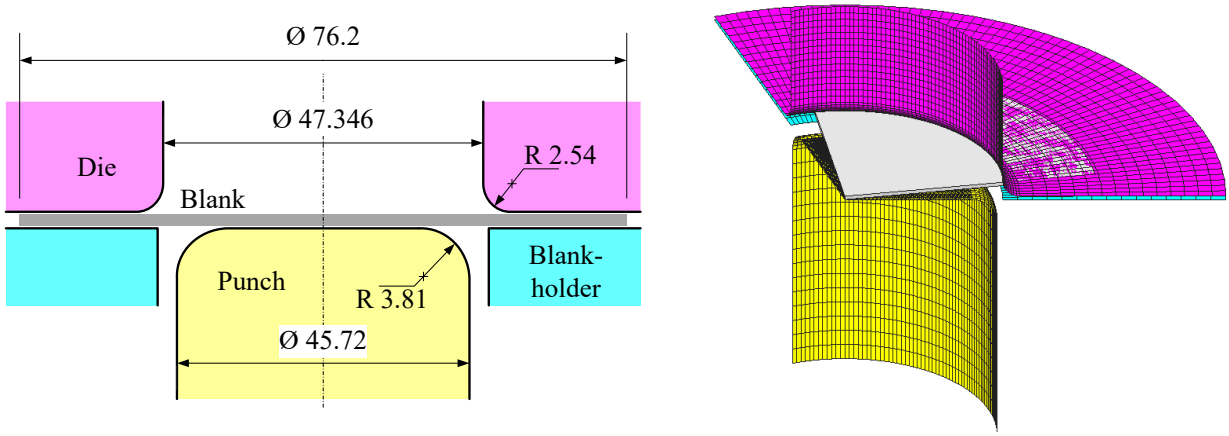


Fig. 1: Definition of the forming process for a cylindrical cup: (a) main dimensions [mm] of the forming tools; (b) discretization of the forming tools using Nagata patches.

The elastic behaviour of this aluminum alloy is assumed isotropic, considering the Young's modulus $E$=70 GPa and the Poisson's ratio $\nu$=0.33. The plastic behaviour is modelled using an isotropic work hardening and is defined by the Swift law, given by:

$$Y = K(\varepsilon_0 + \bar{\varepsilon}^{\mathrm{p}})^n, \tag{1}$$

where $\bar{\varepsilon}^{\mathrm{p}}$ denotes the equivalent plastic strain, while $K$, $\varepsilon_0$ and $n$ are the parameters of the Swift law. The experimental true stress–equivalent plastic strain curve obtained from the uniaxial tensile test performed along the rolling direction was used to fit the parameters of the Swift law, which are listed in Table 1.

Table 1: Parameters used in the Swift law to describe the hardening beahviour of the AA3104.

| $Y_0$ [MPa] | $K$ [MPa] | $n$ | $\varepsilon_0$ |
|---|---|---|---|
| 228.92 | 322.55 | 0.0453 | 0.000516 |

The orthotropic behaviour is modelled by the yield criterion proposed by Plunkett et al. [6], commonly denoted as CPB06ex2. The equivalent stress is written as:

$$\bar{\sigma} = B\left\{\left(|s_1| - ks_1\right)^a + \left(|s_2| - ks_2\right)^a + \left(|s_3| - ks_3\right)^a + \left(|s_1'| - k's_1'\right)^a + \left(|s_2'| - k's_2'\right)^a + \left(|s_3'| - k's_3'\right)^a\right\}^{1/a} \tag{2}$$

where

$$B = \left[1 \Big/ \left\{\left(|\phi_1| - k\phi_1\right)^a + \left(|\phi_2| - k\phi_2\right)^a + \left(|\phi_3| - k\phi_3\right)^a + \left(|\phi_1'| - k'\phi_1'\right)^a + \left(|\phi_2'| - k'\phi_2'\right)^a + \left(|\phi_3'| - k'\phi_3'\right)^a\right\}\right]^{1/a} \tag{3}$$

using

$$\begin{cases} \phi_i = (2/3)C_{i1} - (1/3)C_{i2} - (1/3)C_{i3} \\ \phi_i' = (2/3)C_{i1}' - (1/3)C_{i2}' - (1/3)C_{i3}' \end{cases}, \quad i = 1,2,3 \tag{4}$$

where $s_i$ and $s'_i$ are the principal values of the stress deviatoric component of the Cauchy stress tensor after one and two linear transformations, respectively. The isotropic parameters are $a$ and $k$, while the material anisotropy is defined by the parameters $C_{ij}$ and $C'_{ij}$. The parameter $k$ is equal to zero if the yield stresses in tension and compression are equal ($\sigma^T = \sigma^C$), which is assumed in the present study. The shape of the yield locus is defined by the exponent $a$, which is 8 in this study. Although Eq. (2) presents 18 parameters, it has been shown that the maximum number of independent anisotropic parameters of a 3D orthotropic yield criterion is 17. Thus, it is imposed that $C_{11}$=1.0. In case of metallic, it is not possible to identify the coefficients related with the out of plane shear components, for which it is common to adopt the isotropic value of 1.0.

The calibration of the remaining 13 anisotropy parameters was performed using the in-house code DD3MAT [7], which is based on the minimization of an error function that evaluates the difference between the experimental and predicted values. The set of experimental data used in the calibration of the anisotropy parameters comprises: (i) in-plane distribution of the yield stress and $r$-values extracted from uniaxial tensile tests performed in every 15º to the rolling direction; (ii) data from bulge tests; and (iii) data from disc compression tests. The obtained material anisotropy parameters are listed in Table 2.

Fig. 2 presents the comparison between the numerical and experimental yield stresses and $r$-values. The AA3104 aluminum alloy presents a strong anisotropy of $r$-values, while being almost isotropic in the tensile yield stresses. Globally, the CPB06ex2 yield criterion allows a proper description of both yield stress directionalities and $r$-values. Numerical simulations were also performed considering a von Mises isotropic material with the same hardening behavior as the AA3104 alloy.

Table 2: Parameters used in the CPB06ex2 yield criterion ($a$=8) to describe the anisotropic beahviour of the AA3104.

| $C_{11}$ | $C_{22}$ | $C_{33}$ | $C_{44}$ | $C_{55}$ | $C_{66}$ | $C_{23}$ | $C_{13}$ | $C_{12}$ |
|---|---|---|---|---|---|---|---|---|
| 1.0000 | 0.9498 | 1.1395 | 1.0000 | 1.0000 | -1.2665 | -0.0458 | 0.1658 | -0.0424 |
| $C'_{11}$ | $C'_{22}$ | $C'_{33}$ | $C'_{44}$ | $C'_{55}$ | $C'_{66}$ | $C'_{23}$ | $C'_{13}$ | $C'_{12}$ |
| 1.0094 | 1.2407 | 0.0849 | 1.0000 | 1.0000 | 1.0655 | 0.1402 | -0.4816 | 0.0094 |

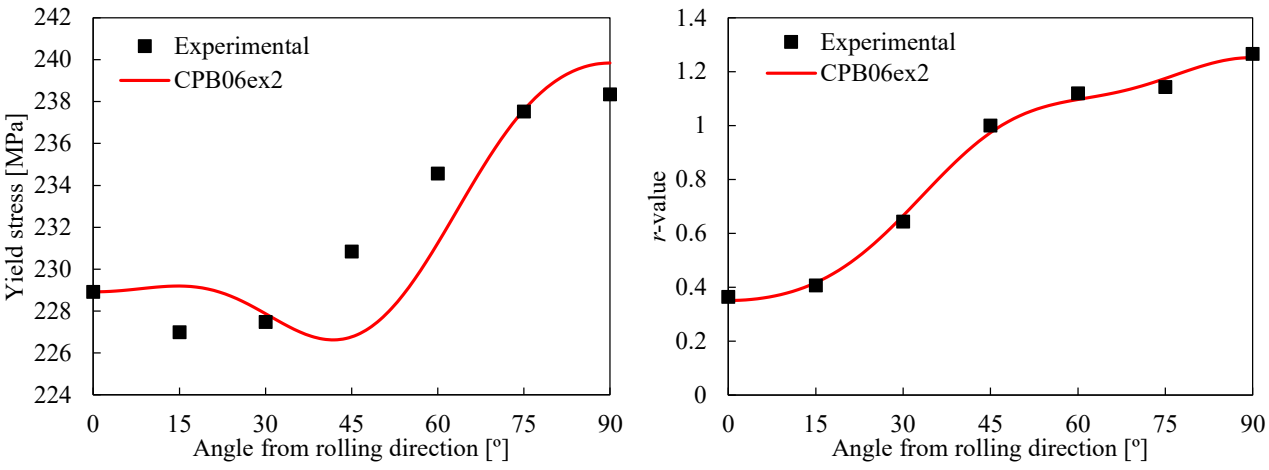


(a) (b)

Fig. 2: Comparison between experimental and predicted: (a) initial uniaxial yield stress; (b) anisotropy coefficient.

## Results and Discussion

The evolution of the predicted punch force evolution is presented in Fig. 3 (a) for three different values of the friction coefficient. An increase of the friction coefficient leads to a global increase in the punch force required to form the cup. The maximum punch force predicted for $\mu$=0.2 is approximately 50% larger than the one predicted under frictionless ($\mu$=0) conditions. On the other hand, the difference between an isotropic material (von Mises) and anisotropic is less than 7%, as highlighted in Fig. 3 (a). The blank-holder force evolution is presented in Fig. 3 (b) for the anisotropic material, highlighting the imposed slightly linear increase. The loss of contact between the blank and

the blank-holder occurs at approximately 20 mm of punch displacement. This value is slightly larger for larger values of friction coefficient, as highlight in the evolution of the force of both tools.

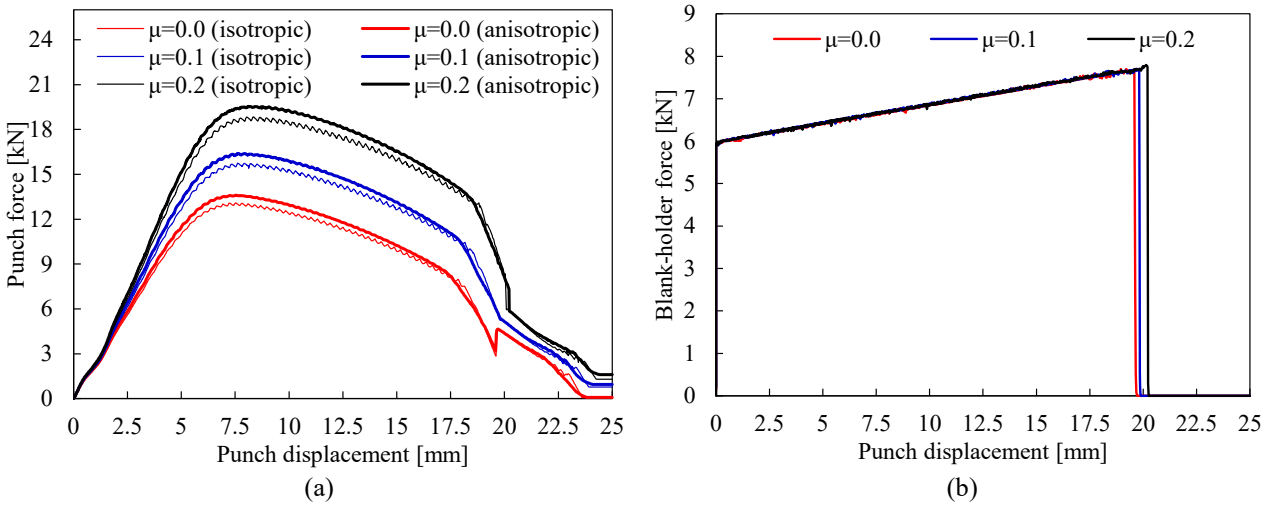


Fig. 3: Effect of the friction coefficient and anisotropy on the numerical prediction: (a) punch force evolution; (b) blank-holder force evolution.

Assuming the material anisotropy defined in Fig. 2, an asymmetrical distribution of the contact forces between the blank and the blank-holder is expected. Fig. 4 (a) presents the distribution of the average normal contact pressure on the blank-holder along the circumferential direction, evaluated for three values of punch displacement. The largest values of normal contact pressure occurs in the transverse direction. Since the area of the flange decreases with the punch displacement while the total blank-holder force presents a slight increase, the average normal contact pressure increases during the punch displacement. Under frictionless conditions, the region with high levels of normal contact pressure is narrower. Also, the maximum value of the average normal contact pressure achieved is at least 50% higher than the one predicted for $\mu$=0.2, evaluated for the same punch displacement. For the same value of punch displacement, the increase of the friction coefficient leads to a larger contact area of the flange, which decreases the normal contact pressure value. The distribution of the average tangential friction pressure on the blank-holder is presented in Fig. 4 (b) for 10 mm of punch displacement and compares three different values of friction coefficient. The location of the largest tangential friction pressure values is identical to the one observed for the normal contact pressure. Moreover, the values are proportional to the friction coefficient adopted.

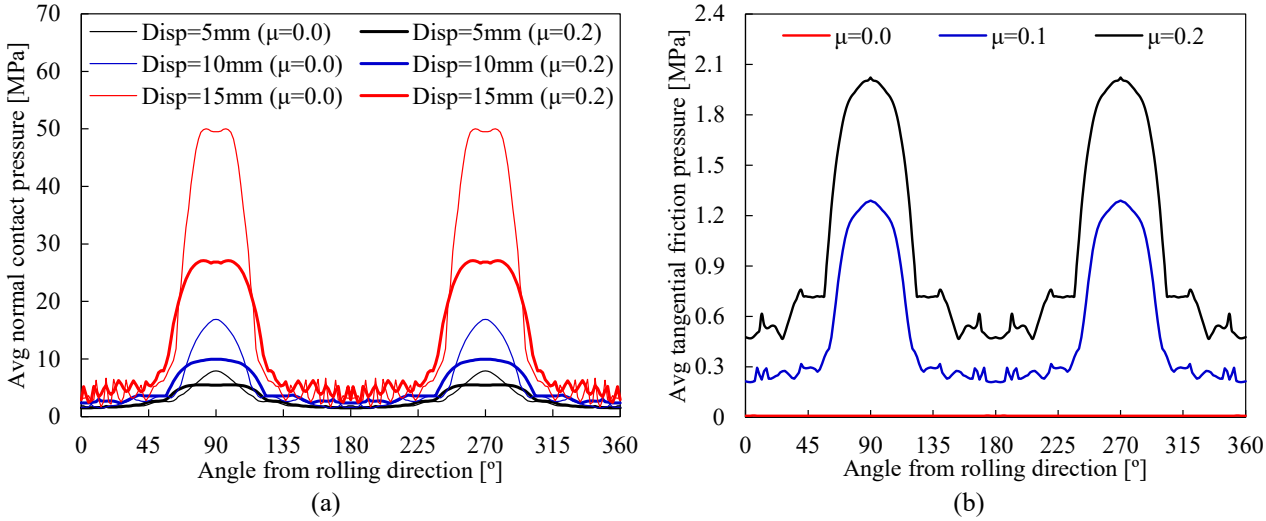


Fig. 4: Distribution of the contact pressure on the blank-holder along the circumferential direction: (a) average normal contact pressure for three values of punch displacement; (b) average tangential friction pressure for 10 mm of punch displacement.

The results presented consider a constant value for the friction coefficient. Nevertheless, it is known that the friction coefficient is affected by several parameters, such as the surface roughness, the amount of lubricant or the contact pressure. Moreover, the machining or finishing/polishing of a tooling surface as well as the rolling process of sheet metals can lead to an anisotropic surface roughness. Therefore, the magnitude and direction of frictional forces acting on a moving body can vary with the direction of sliding, affecting the formability. On the other hand, some authors have reported the reduction of the friction coefficient with the contact pressure [8,9]. Adopting an evolutionary law of that type will make the effect of the non-uniform contact pressure on the earing profile less significant, since the tangential friction pressure becomes more homogeneous.

The asymmetrical distribution of the contact forces between the blank and the blank-holder affects the material flow. The predicted earing profile is presented in Fig. 5 (a) for different values of friction coefficient. Although the cup earing is predominantly dictated by the plastic anisotropy [1,10], the non-uniform contact force distribution changes the earing profile. Indeed, the influence of the friction coefficient on the predicted earing profile is significantly stronger in the transverse direction. Increasing the friction coefficient up to $\mu$=0.2 leads to an increase of cup height of about 0.3 mm in the rolling direction and approximately 1.2 mm in the transverse direction, i.e., around 4 times larger. There is also a visible minor influence of $\mu$ on the earing profile: for frictionless conditions there is a small ear at 0º and none at 90º but, with the increase of $\mu$ the ear at 0º tends to disappear while a small ear develops at 90º. Fig. 5 (a) also shows that the cup height predicted for the isotropic material does not increase linearly with the friction coefficient.

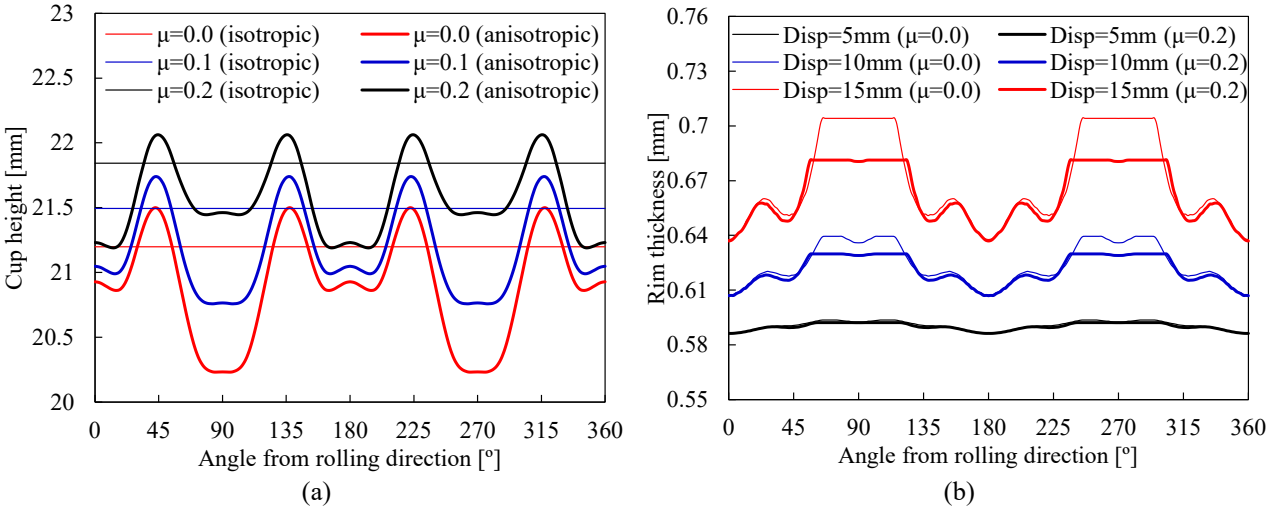


Fig. 5: Numerical prediction: (a) earing profile obtained for different values of friction coefficient; (b) thickness of the flange rim for three values of punch displacement.

Since the flange of the cylindrical cup is under a circumferential compressive stress, the material flow leads to flange thickening. The predicted thickness of the flange rim is presented in Fig. 5 (b) for three values of punch displacement, showing its increase during the cup forming. The maximum thickening always occurs in the transverse direction, which leads to the higher values of normal contact pressure and increased friction forces in that zone (see Fig. 4). The non-uniform thickness distribution along the circumferential direction of the flange is a direct consequence of using a highly anisotropic material, namely the strong in-plane anisotropy of the *r*-value (see Fig. 2). Notice that the transverse direction is subjected to circumferential compression in the rolling direction, which is the direction having the lowest *r*-value. Comparing the frictionless condition with the situation using $\mu$=0.2, the difference in the thickness distribution only occurs around the transverse direction, as highlighted in Fig. 5 (b). In fact, the rim thickness is larger under frictionless conditions due to the absence of friction forces.

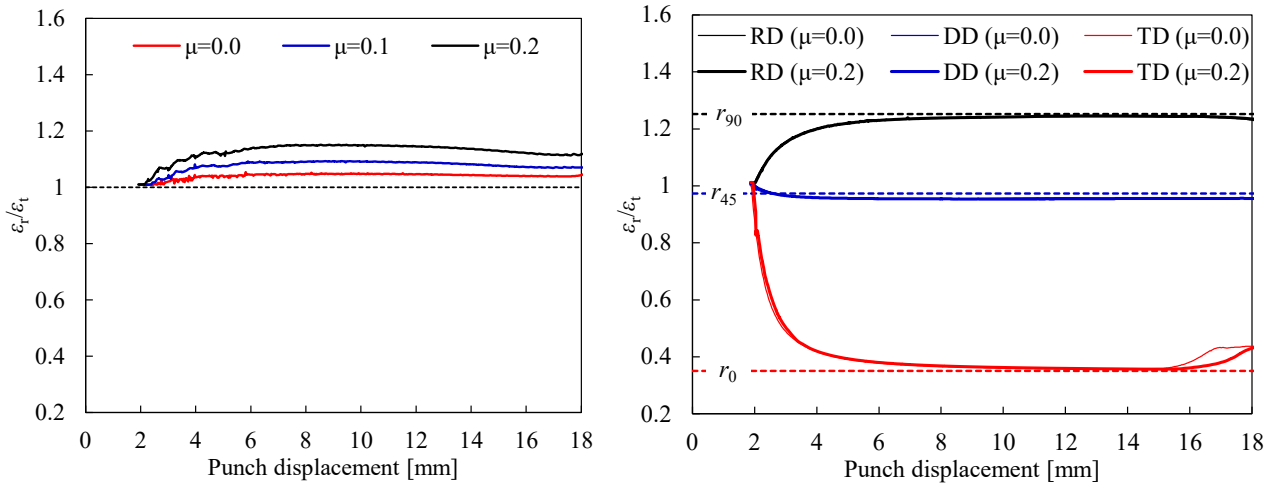


Fig. 6: Ratio between radial strain and thickness strain evaluated in the flange rim: (a) effect of the friction coefficient in an isotropic material; (b) comparison of the strain ratio with the *r*-values estimated with the CPB06ex2 (anisotropic material).

Fig. 6 presents the evolution of the ratio between the plastic strain along the radial and the thickness direction, evaluated in the flange rim from the numerical results. For the isotropic material, the strain ratio $\varepsilon_r/\varepsilon_t$ in the flange rim is slightly higher than 1. This is a consequence of the deviation from the uniaxial compression imposed by the normal contact pressure. This ratio value increases with the friction coefficient, as shown in Fig. 6 (a) and highlights that the friction forces for $\mu$>0 also contributes to the deviation from the uniaxial compression stress state. Considering the anisotropic material defined according to Fig. 2, the strain evolution was measured in three points located in the flange rim, namely in the rolling direction (RD), transverse direction (TD) and diagonal direction (DD). The estimated $\varepsilon_r/\varepsilon_t$ values are in agreement with the *r*-values predicted by CPB06ex2. However, the behaviour of the rim in the direction defined by $\theta$ (to the RD) is controlled by the material compression properties in the direction defined by $\theta$+90º [10]. Thus, the $\varepsilon_r/\varepsilon_t$ evaluated in the RD is compared with the *r*-value at TD and vice-versa, as shown in Fig. 6 (b). Despite the non-uniform distribution of the contact forces between the blank and the blank-holder (see Fig. 4), the entire rim is under uniaxial compression, as highlighted by the proper correlation between the estimated $\varepsilon_r/\varepsilon_t$ values and the *r*-values. The irregular distribution of the contact forces along the radial direction (higher in the middle of the flange) leads to a negligible stress component in the thickness direction at the rim. Nevertheless, the material behaviour is affected by the adjacent region, whose stress states are influenced by the normal component, associated with the contact pressure with the blank-holder, and the shear component, resulting from the friction conditions.

## Conclusions

The earing profile of deep drawn cylindrical cups is related to the anisotropic behavior of the metallic sheet. Nevertheless, the contact conditions between the blank and the blank-holder can also affect the material flow due to the non-uniform distribution of the contact forces in materials with a strong anisotropic behavior of the *r*-values. The influence of the friction conditions on the cup earing trend is numerically assessed in the present study for the AA3104 aluminum alloy. The severe in-plane variation of the plastic anisotropy coefficient leads to an asymmetrical thickness strain distribution in the flange, promoting a non-uniform contact force distribution. The normal contact pressure and consequently the friction force are located mainly around the transverse direction. Therefore, the effect of the friction coefficient on the earing profile is more relevant in this direction. Indeed, the impact of the friction coefficient on the cup height is approximately 4 times larger in the transverse direction in comparison with the effect in the rolling direction. On the other hand, assuming material isotropy, the change of the friction coefficient leads to a simple shift of the earing profile.

**Acknowledgements**

The authors gratefully acknowledge the financial support of the projects POCI-01-0145-FEDER-30592 (PTDC/EME-EME/30592/2017) and UIDB/00285/2020 financed by the Operational Program for Competitiveness and Internationalization, in its FEDER/FNR component, and the Portuguese Foundation of Science and Technology (FCT), in its State Budget component (OE).

**References**

[1] J.H. Yoon, O. Cazacu, J. Whan Yoon, R.E. Dick, Earing predictions for strongly textured aluminum sheets, Int. J. Mech. Sci. 52 (2010) 1563–1578. https://doi.org/10.1016/J.IJMECSCI.2010.07.005.

[2] M. Vrh, M. Halilovič, B. Starman, B. Štok, D.S. Comsa, D. Banabic, Capability of the BBC2008 yield criterion in predicting the earing profile in cup deep drawing simulations, Eur. J. Mech. - A/Solids. 45 (2014) 59–74. https://doi.org/10.1016/J.EUROMECHSOL.2013.11.013.

[3] K. Bouchaâla, M.F. Ghanameh, M. Faqir, M. Mada, E. Essadiqi, Evaluation of the Effect of Contact and Friction on Deep Drawing Formability Analysis for Lightweight Aluminum Lithium Alloy Using Cylindrical Cup, Procedia Manuf. 46 (2020) 623–629. https://doi.org/10.1016/J.PROMFG.2020.03.089.

[4] L.F. Menezes, C. Teodosiu, Three-dimensional numerical simulation of the deep-drawing process using solid finite elements, J. Mater. Process. Technol. 97 (2000) 100–106. https://doi.org/10.1016/S0924-0136(99)00345-3.

[5] D.M. Neto, M.C. Oliveira, L.F. Menezes, J.L. Alves, Applying Nagata patches to smooth discretized surfaces used in 3D frictional contact problems, Comput. Methods Appl. Mech. Eng. 271 (2014) 296–320. https://doi.org/10.1016/j.cma.2013.12.008.

[6] B. Plunkett, O. Cazacu, F. Barlat, Orthotropic yield criteria for description of the anisotropy in tension and compression of sheet metals, Int. J. Plast. 24 (2008) 847–866. https://doi.org/10.1016/J.IJPLAS.2007.07.013.

[7] P.D. Barros, P.D. Carvalho, J.L. Alves, M.C. Oliveira, L.F. Menezes, DD3MAT - A code for yield criteria anisotropy parameters identification., in: J. Phys. Conf. Ser., Institute of Physics Publishing, 2016: p. 32053. https://doi.org/10.1088/1742-6596/734/3/032053.

[8] F. Vollertsen, Z. Hu, Determination of size-dependent friction functions in sheet metal forming with respect to the distribution of the contact pressure, Prod. Eng. 2 (2008) 345–350. https://doi.org/10.1007/S11740-008-0130-4/FIGURES/10.

[9] S. Dou, J. Xia, Analysis of Sheet Metal Forming (Stamping Process): A Study of the Variable Friction Coefficient on 5052 Aluminum Alloy, Met. 2019, Vol. 9, Page 853. 9 (2019) 853. https://doi.org/10.3390/MET9080853.

[10] J.W. Yoon, R.E. Dick, F. Barlat, A new analytical theory for earing generated from anisotropic plasticity, Int. J. Plast. 27 (2011) 1165–1184. https://doi.org/10.1016/j.ijplas.2011.01.002.